Turkish Journal of Electrical Engineering & Computer Sciences

http://journals.tubitak.gov.tr/elektrik/

Research Article

Turk J Elec Eng & Comp Sci
(2015) 23: 1748 – 1760

doi:10.3906/elk-1404-176

MPPT of PV array using stepped-up chaos optimization algorithm

Lihua WANG[1,2,*], Xueye WEI[1], Yuqin SHAO[3], Tianlong ZHU[1], Junhong ZHANG[1]
[1]School of Electronic and Information Engineering, Beijing Jiaotong University, Beijing, P.R. China
[2]School of Electronic Communication & Physics, Shandong University of Science & Technology, Qingdao, P.R. China
[3]Shandong College of Information Technology, Weifang, P.R. China

Received: 11.04.2014 • **Accepted/Published Online:** 20.03.2015 • **Printed:** 30.11.2015

Abstract: In order to achieve maximum efficiency, a maximum power point tracking (MPPT) scheme should be applied in photovoltaic systems. Among all the MPPT schemes, the chaos optimization scheme is one of the hot topics in recent years. In this study, a novel stepped-up chaos optimization algorithm is presented. A chaos mapping $x_{n+1} = \mu \sin(\pi x_n)$ is used as a chaos generator to produce a chaos variable. In the process of MPPT, a coarse search is done to find the current optimal solution in a certain range, and then a fine search reduces the space of optimized variables. Compared with the algorithm of traditional chaos searches, the proposed algorithm is more accurate and can respond quickly. Simulation and experimental results confirm the goodness of the proposed algorithm.

Key words: Stepped-up chaos search, maximum power point tracking, photovoltaic array, optimization algorithm

1. Introduction

Photovoltaic (PV) power generation technology is one of the most important researches in the field of renewable energy, which is significant in theory and practice to mitigate the worldwide energy crisis. The output power of a PV array may vary with solar irradiance, environmental temperature, and load; therefore, maximum power point tracking (MPPT) technology is needed to bring the efficiency of PV arrays into full play [1,2]. It is well known that the output characteristics of PV arrays, which depend on solar irradiance and environmental temperature, are complex and nonlinear. It is difficult to find the mathematical model accurately, and it is also a challenge for a PV system running in an optimum state. Over the past decades, a large number of MPPT methods have been proposed and implemented, including the voltage feedback method [3], perturbation and observation (P&O) method [4,5], power feedback method [6], incremental conductance method [7,8], optimal gradient method [9], artificial neural network method [10], PID/fuzzy control methods [11,12], intermittent control scanning method [13], three-point-weighting method [14], evolutionary algorithm method [15,16], artificial neural network method [17–19], and so on. Every method has its own advantages and disadvantages in enhancing the precision and speed of MPPT control to a certain degree.

Chaos optimization search as a novel method of global optimization has attracted much attention in nonlinear fields [20]. In a traditional chaos optimization algorithm, a single carrier is usually applied to generate the iterative sequence, and then the algorithm can jump out of local maxima effectively. However, the traditional chaos algorithm is usually of low efficiency because it may take a long time to reach the optimal operating

*Correspondence: wanglihua7141@163.com

point at some special state. That means it cannot provide enough speed for the MPPT of PV systems. In order to improve the efficiency of chaos search and overcome the blindness of traditional chaos search, several improved methods have been researched, as follows. Zhou et al. [21,22] proposed a dual carrier chaotic method, selecting two different chaos generations to produce chaos variables. According to the PV system simulations and experiments under different circumstances, this method showed wonderful control effects and robust characteristics. Wang et al. [23] presented a two-stage chaos optimization method. The process of chaos optimization search was divided into two stages: the first stage was based on improved logistic mapping to produce chaos variables and give full play to the ergodicity; the second stage was based on the power function carrier to get a refined search. In this paper, a stepped-up chaos optimization algorithm is applied in the MPPT of a PV system. It applies chaos theory and the iteration formula to produce random and ergodic chaos variables, using them to search for the optimal value in arbitrary precision in continuous variable space. The chaos optimization algorithm is a stochastic search algorithm that differs from all of the existing evolutionary algorithms.

2. PV cell model and characteristics

In the single-diode equivalent model, the individual PV cell is ideally modeled as a current source connected in parallel with a diode, a series resistance, and a shunt resistance, as shown in Figure 1.

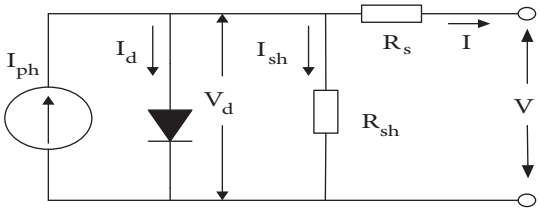

Figure 1. Equivalent circuit of a PV cell.

PV cells are series-connected or parallel-connected to reach the desired voltage and power. Assuming that a PV array consists of N_S PV cells connected in series and N_p cells connected in parallel, and neglecting the influence of the shunt resistance R_{sh}, the $V_{PV} - I_{PV}$ characteristic of a PV array can be described by the following equation [24]:

$$I_{PV} = N_p I_{ph} - N_p I_{sat} \left(\exp \left(\frac{q \left(V_{PV}/N_S + I_{PV} R_s/N_p \right)}{nkT} \right) - 1 \right), \tag{1}$$

where I_{ph} is the light-generated current, I_{sat} denotes the reverse saturation current, R_s is the series resistance of the PV module, n is the diode ideality factor, k is Boltzmann's constant, T is the cell absolute temperature, and q is the electron charge; their values can be referenced in [17,19].

It is straightforward to obtain the PV array power:

$$P_{PV} = N_p I_{ph} V_{PV} - N_p I_{sat} V_{PV} \left(\exp \left(\frac{q \left(V_{PV}/N_S + I_{PV} R_s/N_p \right)}{nkT} \right) - 1 \right). \tag{2}$$

From Eqs. (1) and (2), it is clear that the output characteristics of the PV array are highly nonlinear, affected by the variation of internal parameters and external environmental factors such as light-generated current, reverse saturation current, series resistance, temperature, irradiance, and load.

The current–voltage ($I_{PV}-V_{PV}$) and power–voltage ($P_{PV}-V_{PV}$) curves of the PV array under different irradiances are shown in Figures 2a and 2b. The $I_{PV}-V_{PV}$ and $P_{PV}-V_{PV}$ curves of the PV array under different environmental temperatures are illustrated in Figures 2c and 2d. Obviously, the maximum power changes along with the variation of irradiance and temperature. Furthermore, there exists a unique operating point where the PV array has a maximum power output.

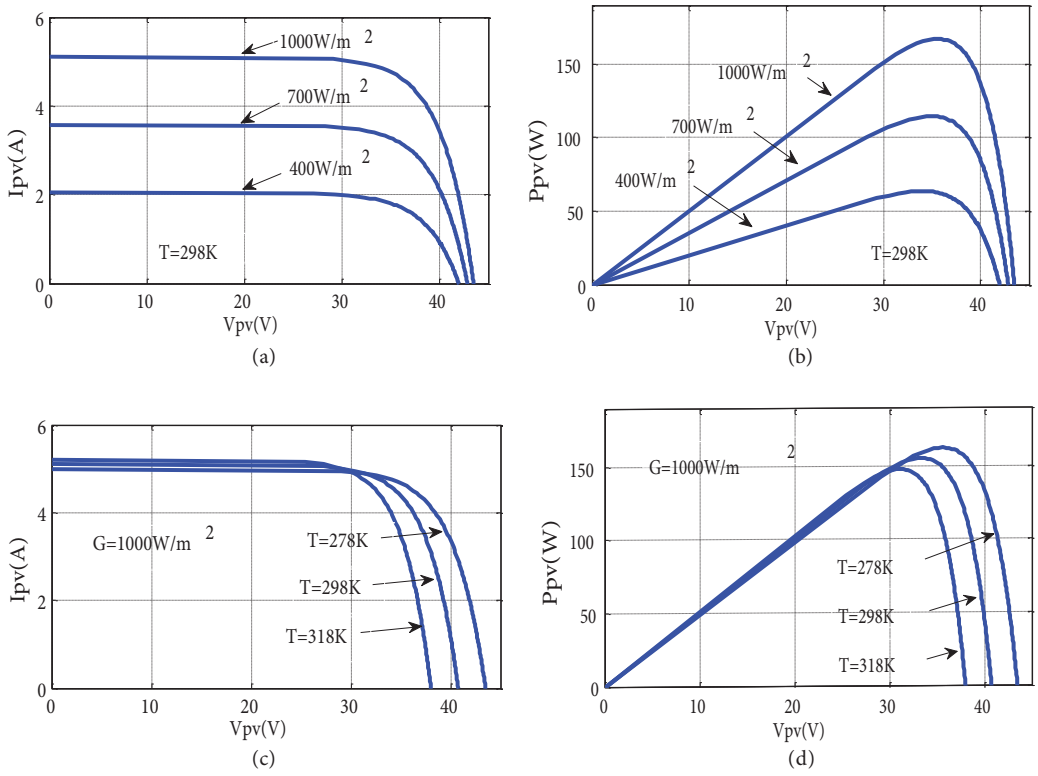

Figure 2. (a) $I_{PV}-V_{PV}$ and (b) $P_{PV}-V_{PV}$ curves of PV module under different irradiances. (c) $I_{PV}-V_{PV}$ and (d) $P_{PV}-V_{PV}$ curves of PV module under different environmental temperatures.

3. Chaos optimization search

3.1. Chaos mapping

In most of the chaos optimization algorithms, chaos variables are generated by logistic mapping [22,23], but the uneven distribution (denser at the ends and sparser in the center) will weaken the ergodicity of chaos variables. To overcome this problem, a new chaos mapping is given here, as demonstrated in Eq. (3):

$$x_{n+1}=\mu\sin(\pi x_n)\quad n=1,2,3..., \tag{3}$$

where μ is a control parameter. Setting $\mu=2$, Eq. (3) is completely in chaos condition, and x_n is ergodic within [–2, 2]. The bifurcation diagram of $x_{n+1}=\mu\sin(\pi x_n)$ is shown in Figure 3a. Using the iterated function, any variable in the optimization space can be obtained, as depicted in Figure 3b.

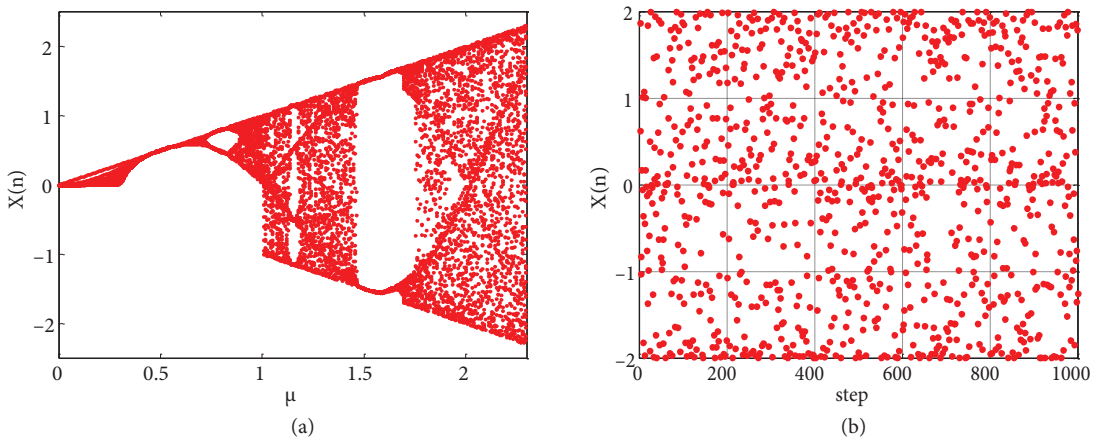

Figure 3. Bifurcation diagram and iterative sequence of $x_{n+1} = \mu \sin(\pi x_n)$ mapping: (a) bifurcation diagram, (b) iterative sequence ($\mu = 2$).

3.2. Chaos optimization search for MPPT

The chaos optimization method is an effective way to solve the optimization problem of a nonlinear multimodal function with boundary constraint. The function can be described as follows [25]:

$$f = f(x_i^*) = \max f(x_i) \quad i = 1, 2, 3...N \quad x_i \in [c_i, d_i], \tag{4}$$

where x_i is an optimization variable, a vector whose dimension is equal to the parameter number of the optimization problem. Here it represents the output voltage of the PV array. c_i and d_i are the lower and upper limits of x_i; N is the number of x_i; $f(x_i)$ is the mathematical model of optimization problems, which is equivalent to the fitness function. In this paper, it is the output power of the PV array. $f(x_i^*)$ is the maximum output power of the PV array, and x_i^* is the output voltage of the maximum power point.

It is difficult for the traditional chaos search, which is related to the complexity of the objective function, to determine the time of the search. Therefore, the traditional chaos search cannot guarantee the quality of the search [26,27]. In this paper, in order to make the chaos search more efficient, a new stepped-up chaos optimization method is proposed: the rough search is used to find the current optimal solution in a certain range; the fine search is used to reduce the search space of optimized variables and improve the convergence speed. The proposed chaos search algorithm is described as follows:

Step1: Initialization

Set $k = 0$, $k' = 0$, $c = 0$, $d = 50$, $p^* = 0$, and $r = 0$. k is the number of iterations in the coarse search, $k = 0, 1, 2, \cdots, n$. k' is the number of iterations in the fine search. c and d are the lower and upper limits of the output voltage range, respectively. p^* is the objective function; here, it is the maximum output power of a PV array. r is the number of iterations while p^* is kept at a constant value. $x_i(0)$ are the different initial values within [–2, 2], $i = 0, 1, 2, \cdots, m$.

Step2: Mapping chaos variables to optimization variables

The chaos variable $x_i(k) \in [-2, 2]$ produced by Eq. (3) must be transformed into the solution space (namely, the output voltage range of PV array), and the transform equation can be described as follows:

$$x_i'(k) = c_i + d_i \frac{(x_i(k) + 2)}{4}, \tag{5}$$

where c_i and d_i are the parameters whose initial values are related to $[c,d]$, and c and d are the boundary values of output voltage as previously mentioned. The initial values of c_i and d_i can be written as follows:

$$c_i = c; \quad d_i = d - c. \tag{6}$$

Step3: First chaos optimization search (coarse search)

If $p(k) > p^*$, then $p^* = p(k)$, $x_i^* = x_i'(k)$, or else abandon $x_i'(k)$, $r = r + 1$. Then $k = k + 1$, loop until $r > 6$ or $k > 100$.

Step4: Second chaos optimization search (fine search)

Take $x_i''(k')$ as a new chaos variables according to Eq. (7), where x_i^* is the current optimal solution of the first chaos optimization search, h_i is the regulation constant of the fine search, and $x(k')$ is a chaos variable produced by Eq. (3). If $p(k') > p^*$, then $p^* = p(k')$, $x_i^* = x_i''(k')$, or else abandon $x_i''(k')$, $r = r + 1$. Then $k' = k' + 1$, loop until $r > 6$ or $k > 100$.

$x_i''(k') = x_i^* + h_i \times x(k')$

Step5: Reduce search space and improve convergence speed

Take the current optimal solution x_i^* as the center, adjusting the boundary value of c and d to reconstruct the value range of optimization variables. The process is as follows:

Suppose the distance $L_{xc} = x_i^* - c$ and $L_{xd} = d - x_i^*$. In the next search, the new search space is $[c', d']$, the center is x_i^*, and the radius is $\min(L_{xa}, L_{xb})/\alpha$. Then:

$$\begin{aligned} c' &= x_i^* - \min(|c - x_i^*|, |d - x_i^*|)/\alpha, \\ d' &= x_i^* + \min(|c - x_i^*|, |d - x_i^*|)/\alpha, \end{aligned} \tag{7}$$

where α is a constant , $\alpha \geq 1$. According to Eq. (6), the new values of c_i' and d_i' can be written as follows:

$$c_i' = c'; \quad d_i' = d' - c'. \tag{8}$$

According to Eqs. (7) and (8), we can get:

$$\begin{aligned} c_i' &= x_i^* - \min(|c - x_i^*|, |d - x_i^*|)/\alpha, \\ d_i' &= 2 \times \min(|c - x_i^*|, |d - x_i^*|)/\alpha. \end{aligned} \tag{9}$$

Consider the following:

$$c = c_i; \quad d = c_i + d_i.$$

The equation for reducing the search space is:

$$\begin{aligned} c_i' &= x_i^* - \min(|c_i - x_i^*|, |d_i + c_i - x_i^*|)/\alpha, \\ d_i' &= 2 \times (\min(|c_i - x_i^*|, |d_i + c_i - x_i^*|)/\alpha), \\ h_i &= h_i/\beta, \end{aligned} \tag{10}$$

where α and β are constants. Here, $\alpha = \beta = 2.1$. Then go to Step2.

Step6: If the number of loops l is greater than 3, then stop the chaos search process. Finally, x_i^* is the optimal output voltage at the MPP, and p^* is the maximum output power.

The block flow diagram of the MPPT process is depicted in Figure 4.

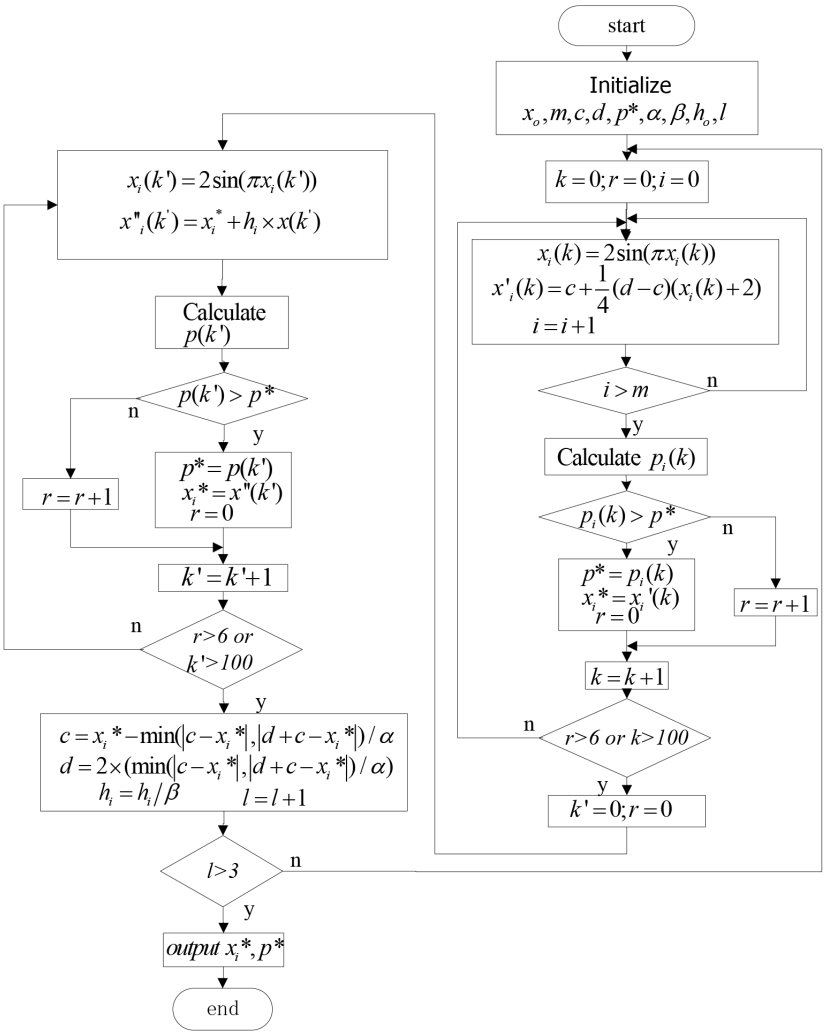

Figure 4. Block flow diagram of MPPT.

4. Simulation experiment

4.1. Simulation model

According to the mathematical model, the model of a PV cell is built by MATLAB/Simulink, as shown in Figure 5. The simulation prototype is the single-crystal silicon whose type is JSM120W, made by JESENSOLAR, Qingdao. The parameters are given as follows: STC (Standard Test Condition: solar irradiance is 1000 W/m^2, environmental temperature is 298 K) open-circuit voltage $U_{oc,ref}$ = 52.1 V; STC MPP voltage $U_{mp,ref}$ = 44.5 V; STC short-circuit current $I_{sc,ref}$ = 2.92 A; STC MPP current $I_{mp,ref}$ = 2.64 A; short-circuit current variation coefficient with change of temperature $\mu_{I,ref}$ = 0.12%/°C = 0.003504 A/°C; open-circuit voltage change of temperature $\mu_{v,ref}$ = –126.79 mV/°C.

To adjust the PV array output voltage for maximizing the solar power generation, a DC/DC boost converter is connected in the PV system as shown in Figure 6.

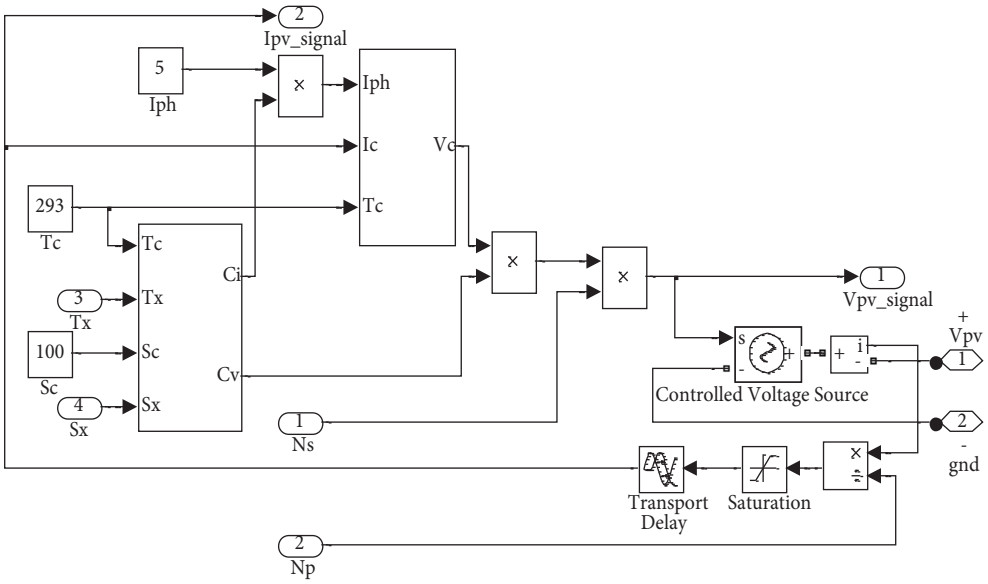

Figure 5. The simulation model of a PV array.

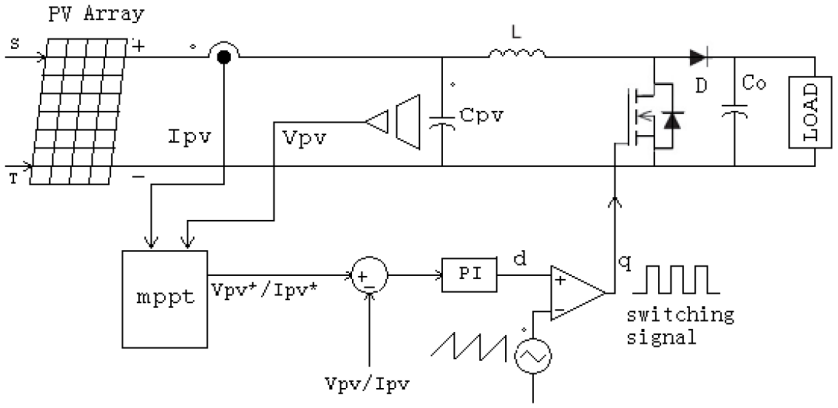

Figure 6. The block diagram of a PV system comprising MPPT and boost converter.

4.2. Tracking simulation of step response

Comparing the results of the proposed method with the traditional single carrier chaos search and P&O search, which are commonly used, the step response tracking results are shown in Figure 7. According to the simulation results, in Figure 7a, the P&O search tracked rapidly; it takes less than 0.02 s to reach the operating point, but it has an inherent voltage ripple on the output of a PV system. In Figure 7b, the single carrier chaos search tracked steadily but slowly, at more than 0.07 s, and in Figure 7c, the proposed method just needed about 0.03 s to reach the tracking object and make the system operate steadily.

4.3. Simulation results

4.3.1. Simulation with rapid change (step change)

The output performances of the PV array under rapid changes are shown in Figures 8–11. Figure 8 shows the simulation of irradiance increase: at the beginning, the irradiance is 700 W/m^2, and output power is controlled at 75.82 W (40.02 V, 1.893 A). At t = 1.25 s, a step change is added, and the irradiance is changing from

700 W/m^2 to 800 W/m^2 while the output power is promptly varying to 89.81 W (41.90 V, 2.145 A). At t = 2.5 s, the irradiance is changing from 800 W/m^2 to 900 W/m^2 and the output power is rapidly turning into 103.51 W (43.71 V, 2.373 A); at t = 3.75 s, the irradiance is changing from 900 W/m^2 to 1000 W/m^2 and the output power is quickly rising to 116.11 W (44.71 V, 2.597 A). Figure 9 shows the simulation results under the irradiance decrease condition, where the changing trends are opposite those in Figure 8. When the irradiance is 1000 W/m^2, the output power is about 116.11 W (44.71 V, 2.597 A), which is close to STC MPP (44.90 V, 2.589 A), and the error is 0.12% (compared with the STC MPP 116.25 W).

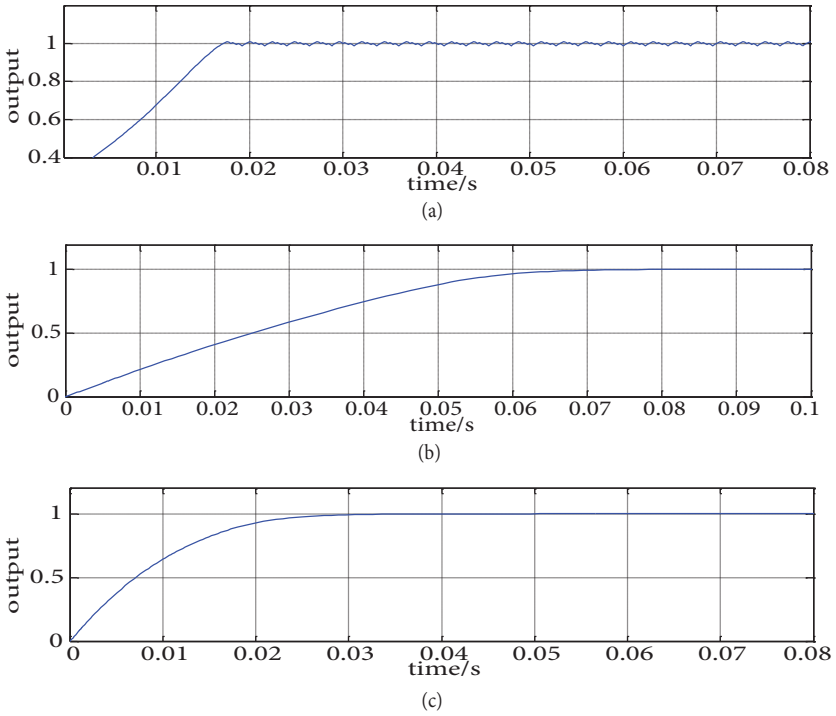

Figure 7. Tracking control results diagram of step response by some methods: (a) P&O, (b) single chaos, (c) stepped-up chaos.

Figures 10 and 11 show the output performance of the PV array under rapid temperature change while the irradiance is 1000 W/m^2. Figure 10 shows the simulation results of temperature rising: the temperature is changing from 273 K to 283 K at t = 1 s, changing from 283 K to 293 K at t = 2 s, and changing from 293 K to 303 K at t = 3 s, and then it continues changing from 303 K to 313 K at t = 4 s. Figure 11 illustrates the simulation results of the temperature dropping; the simulation shows a contrary tendency to Figure 10.

4.3.2. Simulation with slow change (sinusoidal variation)

Figures 12 and 13 show the output performance of the PV array with the slow change of irradiance and temperature. In Figure 12, the temperature remains constant at 298 K, and the irradiance has a sinusoidal change whose period is 5 s. In Figure 13, the irradiance remains constant at 1000 W/m^2, and the temperature also has a sinusoidal change from 273 K to 313 K.

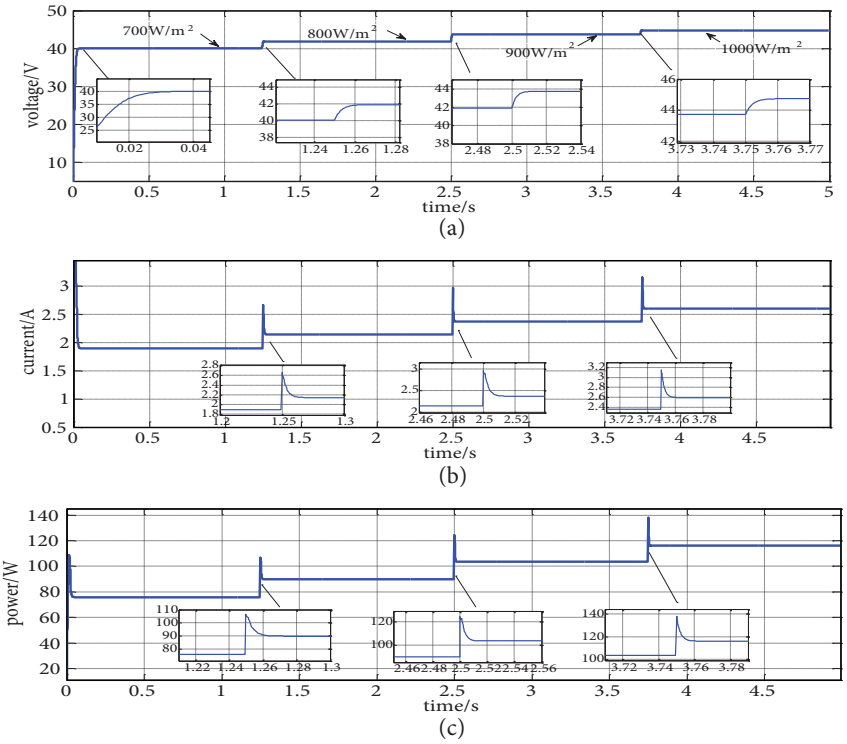

Figure 8. Simulation results with irradiance increasing rapidly (T = 298 K): (a) voltage, (b) current, (c) power.

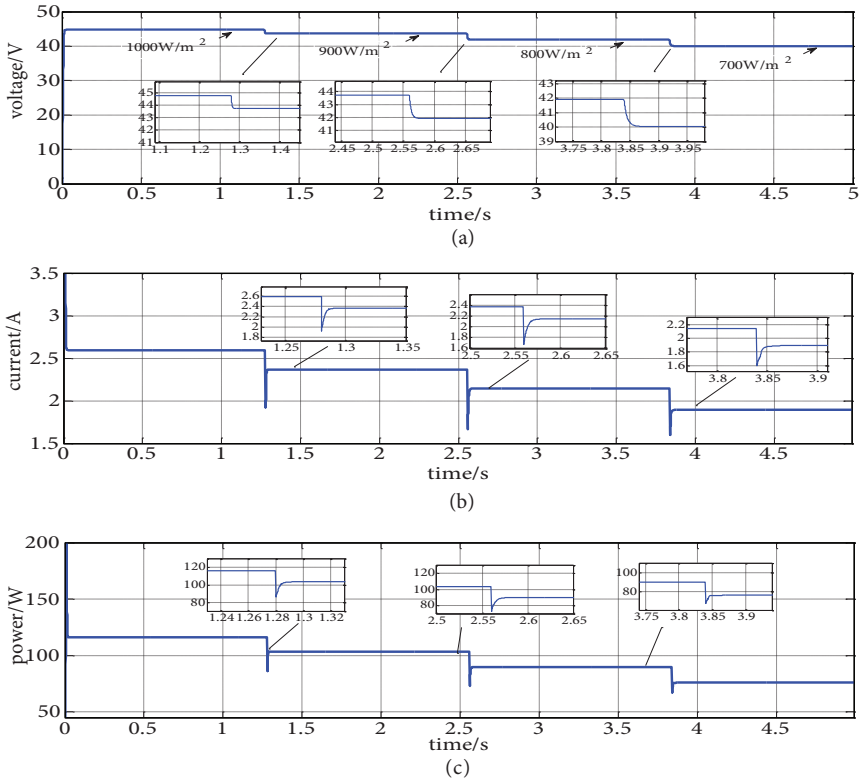

Figure 9. Simulation results with irradiance decreasing rapidly (T = 298 K): (a) voltage, (b) current, (c) power.

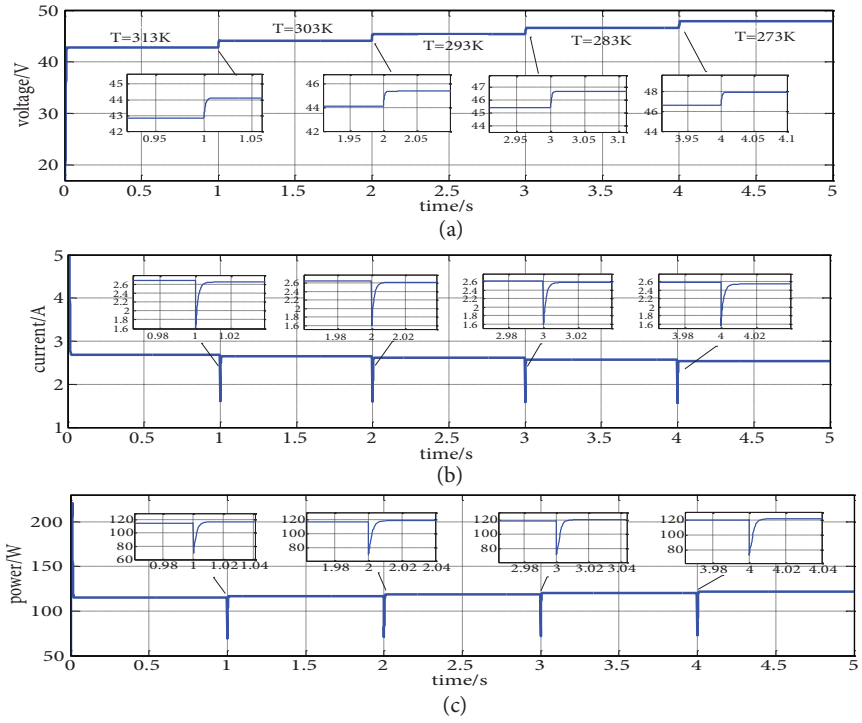

Figure 10. Simulation results with temperature dropping rapidly (G = 1000 W/m^2): (a) voltage, (b) current, (c) power.

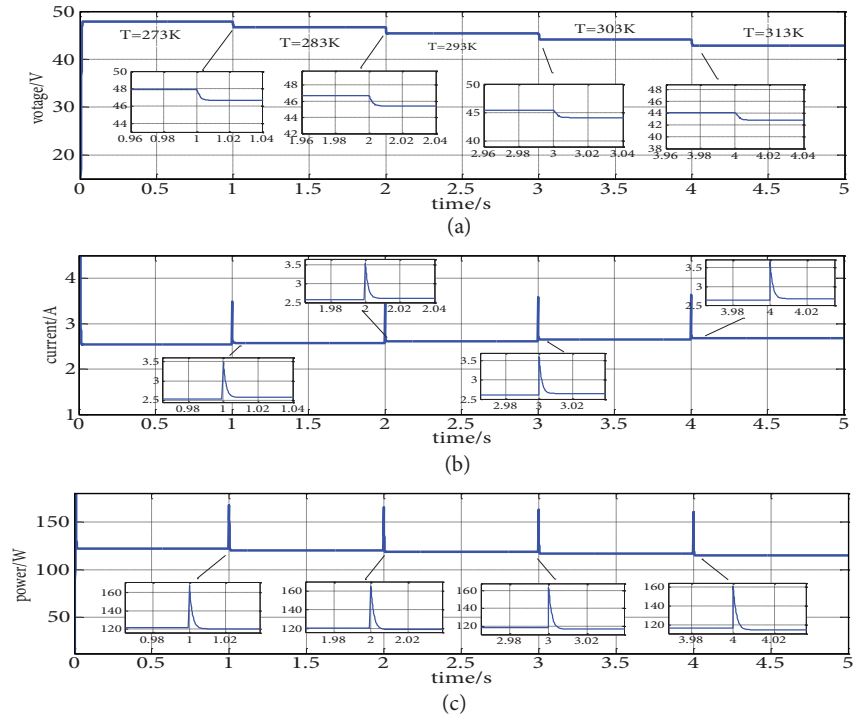

Figure 11. Simulation results with temperature rising rapidly (G = 1000 W/m^2): (a) voltage, (b) current, (c) power.

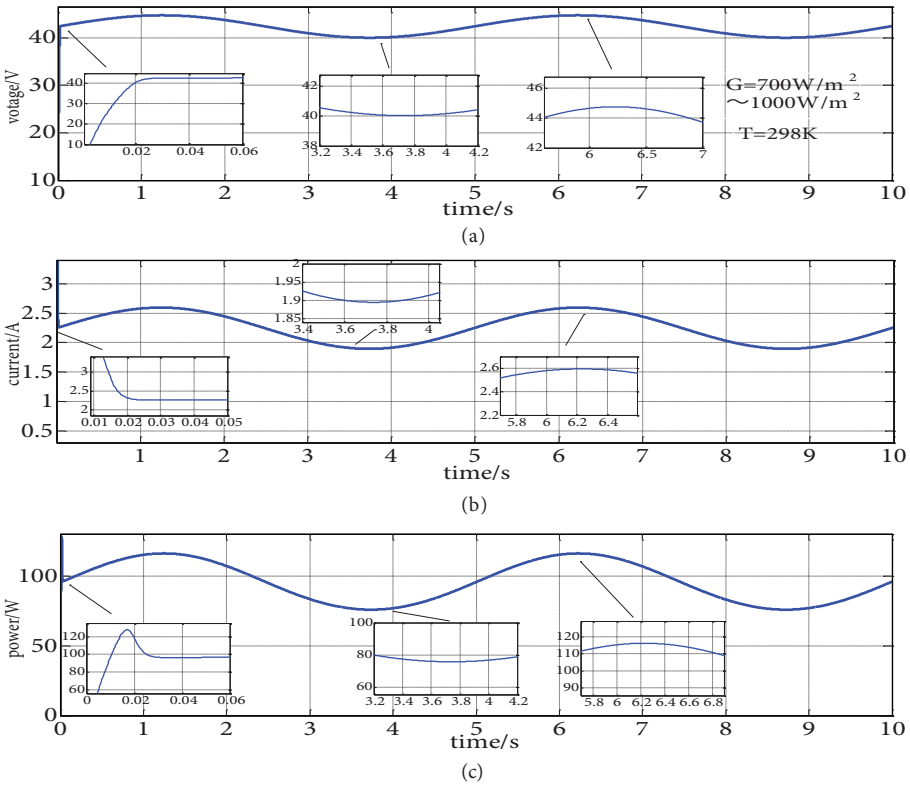

Figure 12. Simulation results with irradiance changing slowly: (a) voltage, (b) current, (c) power.

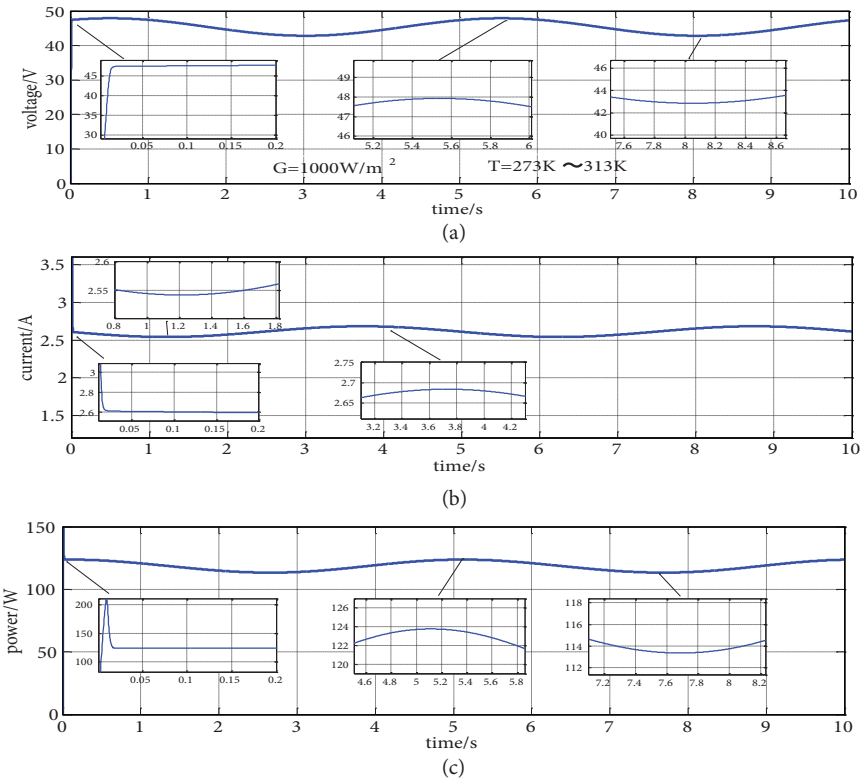

Figure 13. Simulation results with temperature changing slowly: (a) voltage, (b) current, (c) power.

From Figures 8–13, we can see that, while the environmental conditions change, the voltage and current of the PV array quickly respond and overshoot less; the PV system will rapidly track the change smoothly and ultimately steadily around the new MPP.

5. Conclusion

A stepped-up chaos optimization algorithm that is the first to apply MPPT for a PV system has been proposed. In this paper, $x_{n+1} = \mu \sin(\pi x_n)$ is adopted as the carrier to produce chaos variables. Comparing the results of MPPT with the traditional single chaos and P&O methods, the proposed algorithm may increase the efficiency of the chaos search and overcome the blindness of the traditional chaos search. The simulation model is built by MATLAB/Simulink. Compared with the theoretical value of maximum output power of the PV array, the error of the proposed method is about 0.12%, and the proposed method has fast tracking response and valuable performance. In a sequel paper, we will provide experimental results of MPPT under the proposed method.

Acknowledgments

This work was supported by the National Natural Science Foundation of China under Grant 61471224 and by the Union Innovation Funds Project of Jiangsu Province, China, under Grant BY2013068.

References

[1] Enslin J. Maximum power point tracking: a cost saving necessity in solar energy systems. Renew Energ 1992; 2: 543–549.

[2] Salas V, Olías E, Barrado A, Lázaro A. Review of the maximum power point tracking algorithms for stand-alone photovoltaic systems. Sol Energ Mat Sol C 2006; 90: 1555–1578.

[3] Maheshappa HD, Nagaraju J, Murthy MV. An improved maximum power point tracker using a step-up converter with current locked loop. Renew Energ 1998; 13:195–201.

[4] Houssamo I, Locment F, Sechilariu M. Experimental analysis of impact of MPPT methods on energy efficiency for photovoltaic power systems. Int J Electr Power Energy Syst 2013; 46: 98–107.

[5] Liu FR, Kang Y, Zhang Y, Duan SX. Comparison of P&O and hill climbing MPPT methods for grid-connected PV converter. In: Proceedings of the 3rd IEEE Conference on Industrial Electronics and Applications; 3–5 June 2008; Singapore. New York, NY, USA: IEEE. pp. 804–807.

[6] Nafeh AA, Fahmy FH, Mahgoub OA, El-Zahab EM. Developed algorithm of maximum power tracking for stand-alone photovoltaic system. Energ Sources 1998; 20: 45–53.

[7] Harada K, Zhao G. Controlled power interface between solar cell and ac source. IEEE T Power Electr 1993; 8: 654–662.

[8] Li JY, Wang HH. Maximum power point tracking of photovoltaic generation based on the optimal gradient method. In: Asia-Pacific Power and Energy Engineering Conference; 27–31 March 2009; Wuhan, China. New York, NY, USA: IEEE. pp. 692–695.

[9] Yang SY, Wu LH, Liu ZX. Research on photovoltaic grid-connected generation system. In: International Conference on Manufacturing Science and Technology; 16–18 September 2011; Singapore. New York, NY, USA: IEEE. pp. 383–390.

[10] Kassem AM. MPPT control design and performance improvements of a PV generator powered DC motor-pump system based on artificial neural networks. Int J Electr Power Energy Syst 2012; 43: 90–98.

[11] Chiu CS, Li ZH, Chen, YH. T-S fuzzy direct maximum power point tracking of wind energy conversion systems. Int J Fuzzy Syst 2013; 15: 192–202.

[12] Al-Nabulsi A, Dhaouadi R. Efficiency optimization of a DSP-based standalone PV system using fuzzy logic and dual-MPPT control. IEEE T Ind Inform 2012; 8: 573–584.

[13] Dounis AI, Kofinas P, Alafodimos C. Adaptive fuzzy gain scheduling PID controller for maximum power point tracking of photovoltaic system. Renew Energ 2013; 60: 202–214.

[14] Jiang JA, Huang TL, Hsiao YT, Chen CH. Maximum power point tracking for photovoltaic power system. Tamkang J Sci Eng 2005; 8: 147–153.

[15] Adly M, Besheer AH. A meta-heuristics search algorithm as a solution for energy transfer maximization in stand-alone photovoltaic systems. Int J Elec Power 2013; 51: 243–254.

[16] Ishaque K, Salam Z. A review of maximum power point tracking techniques of PV system for uniform insolation and partial shading condition. Renew Sust Energ Rev 2013; 19: 475–488.

[17] Bishop JW. Computer simulation of the effects of electrical mismatches in photovoltaic interconnection circuits. Sol Cells 1988; 25: 73–89.

[18] Riad K, Horia A, Jean PG, Traian I, Gérard C, Paul A. Modeling of the photovoltaic cell circuit parameters for optimum connection model and real-time emulator with partial shadow conditions. Energy 2012; 42: 57–67.

[19] Gow JA, Manning CD. Development of a photovoltaic array model for use in power-electronics simulation studies. IEE P-Elect Pow Appl 1999; 146: 193–200.

[20] Arora JS, Elwakeil OA, Chahande AI, Hsieh CC. Global optimization methods for engineering application: a review. Struct Optimization 1995; 9: 137–159.

[21] Zhou L, Chen Y, Liu Q, Wu J. Maximum power point tracking (MPPT) control of a photovoltaic system based on dual carrier chaotic search. J Control Theory Appl 2012; 10: 244–250.

[22] Zhou L, Chen Y, Guo K, Jia FC. New approach for MPPT control of Photovoltaic system with mutative-scale dual-carrier chaotic search. IEEE T Power Electr 2011; 26: 1038–1048.

[23] Wang LH, Wei XY, Zhu TL, Zhang JH. Two-stage chaos optimization search application in maximum power point tracking of PV array. Math Probl Eng 2014: 2014; 464835.

[24] Celik AN, Acikgoz N. Modelling and experimental verification of the operating current of mono-crystalline photovoltaic modules using four- and five-parameter models. Appl Energy 2007; 84: 1–15.

[25] Salas OH, Banks SP. Optimal control of chaos in nonlinear driven oscillators via linear time-varying approximations. Int J Bifurcat Chaos 2008; 18: 3355–3374.

[26] Yang DX, Li G, Cheng GD. On the efficiency of chaos optimization algorithms for global optimization. Chaos Solitons Fract 2007; 34: 1366–1375.

[27] Li LX, Yang YX, Peng H, Wang XD. An optimization method inspired by "chaotic" ant behavior. Int J Bifurcat Chaos 2006; 16: 2351–2364.